Electronic Supplementary Material (ESI) for Dalton Transactions.

Electronic Supplementary Information

A Yolk-Shell Structure Construction for Metal-Organic Framework toward an Enhanced Electrochemical Water Splitting Catalysis

Zhenhang Xu, Wei Zuo, Qiuxiang Mou, Gongzhen Cheng, Huaming Zheng and Pingping Zhao

Table of contents

1. Supplementary Figures

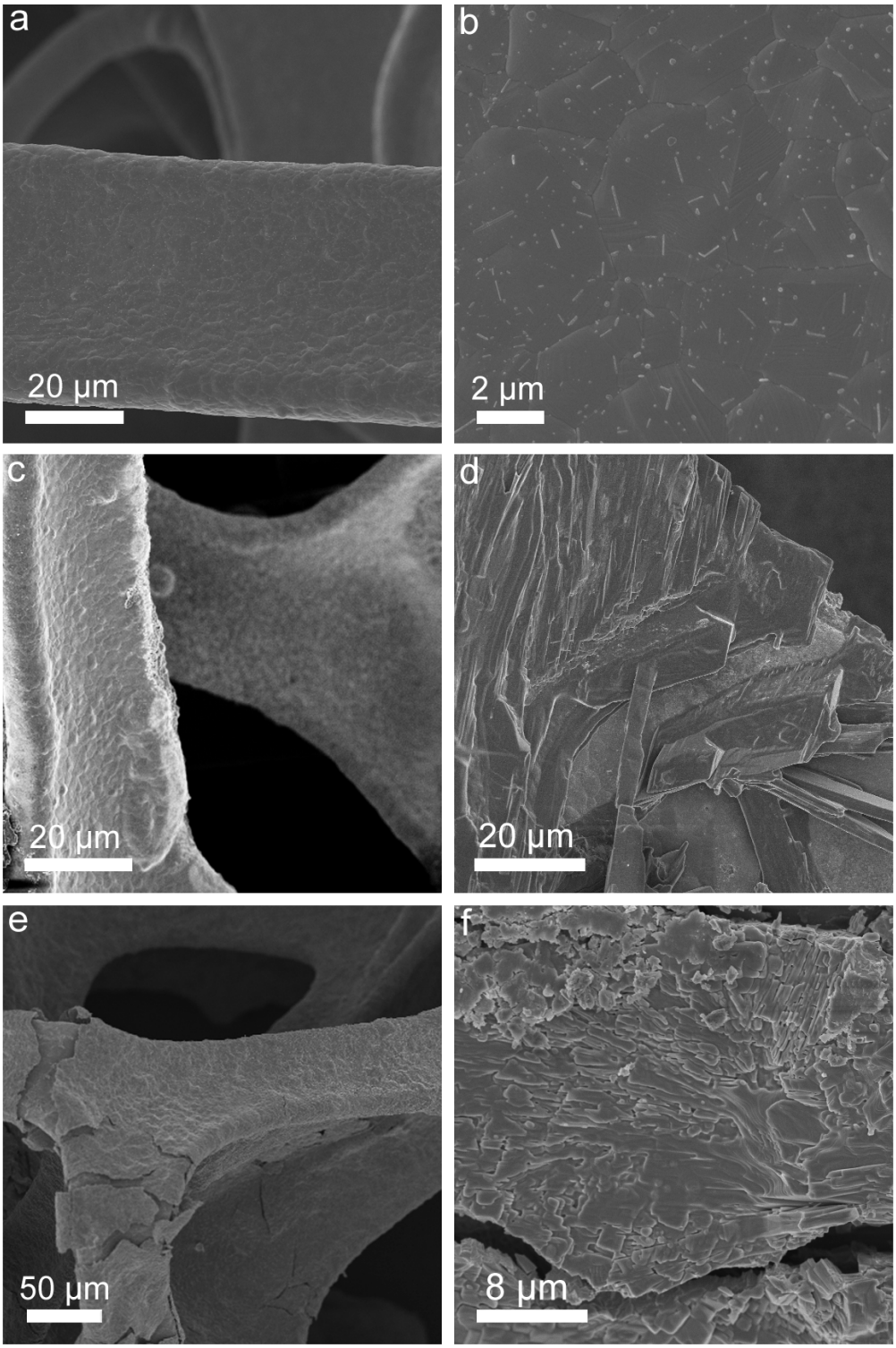

Figure S1. (a), (b): FESEM image of nickel foam; (c), (d): FESEM image of nickel foam after oxidation; (e), (f): FESEM image of nickel foam after oxidation and phosphorization treatment.

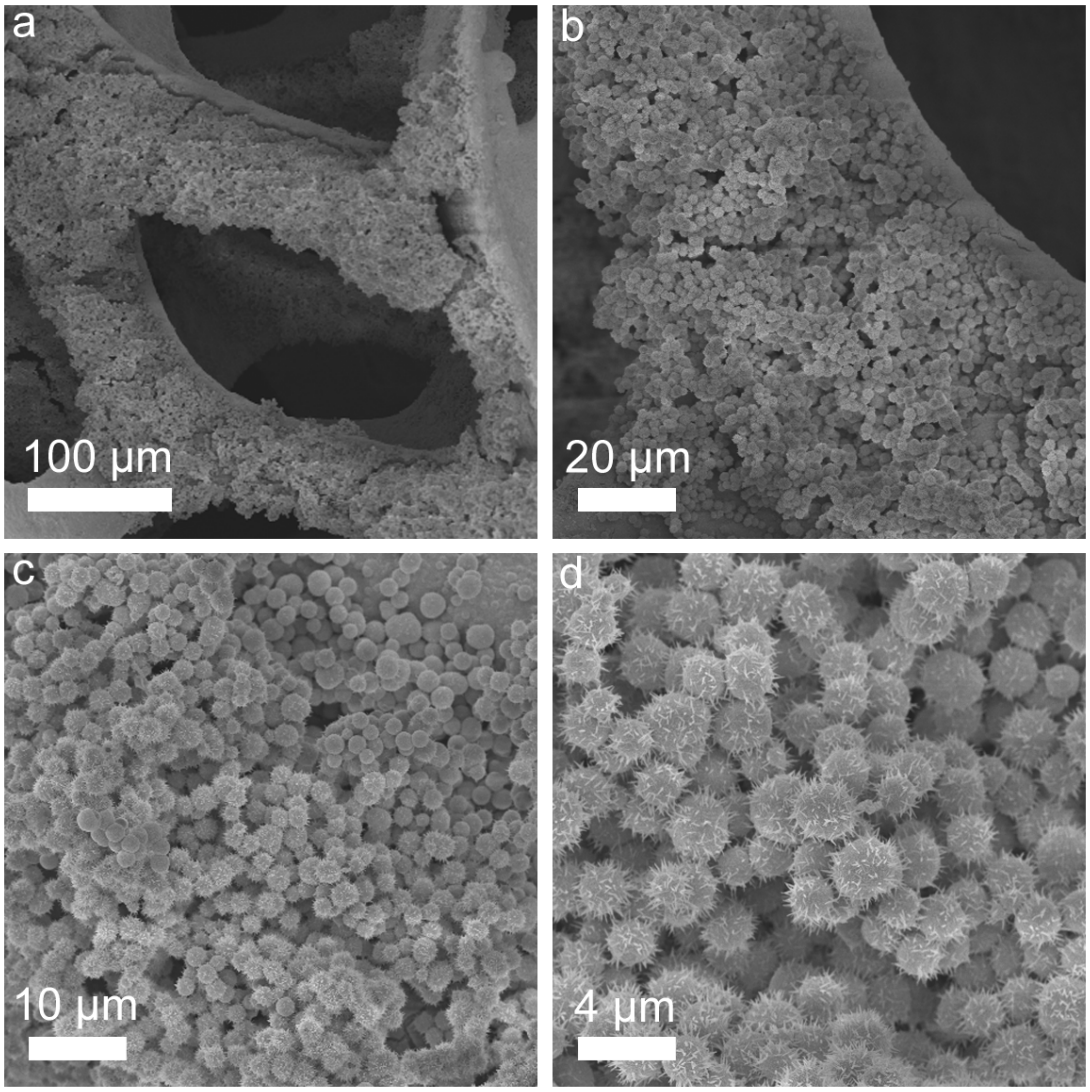

Figure S2. FESEM image of synthetic Ni MOF.

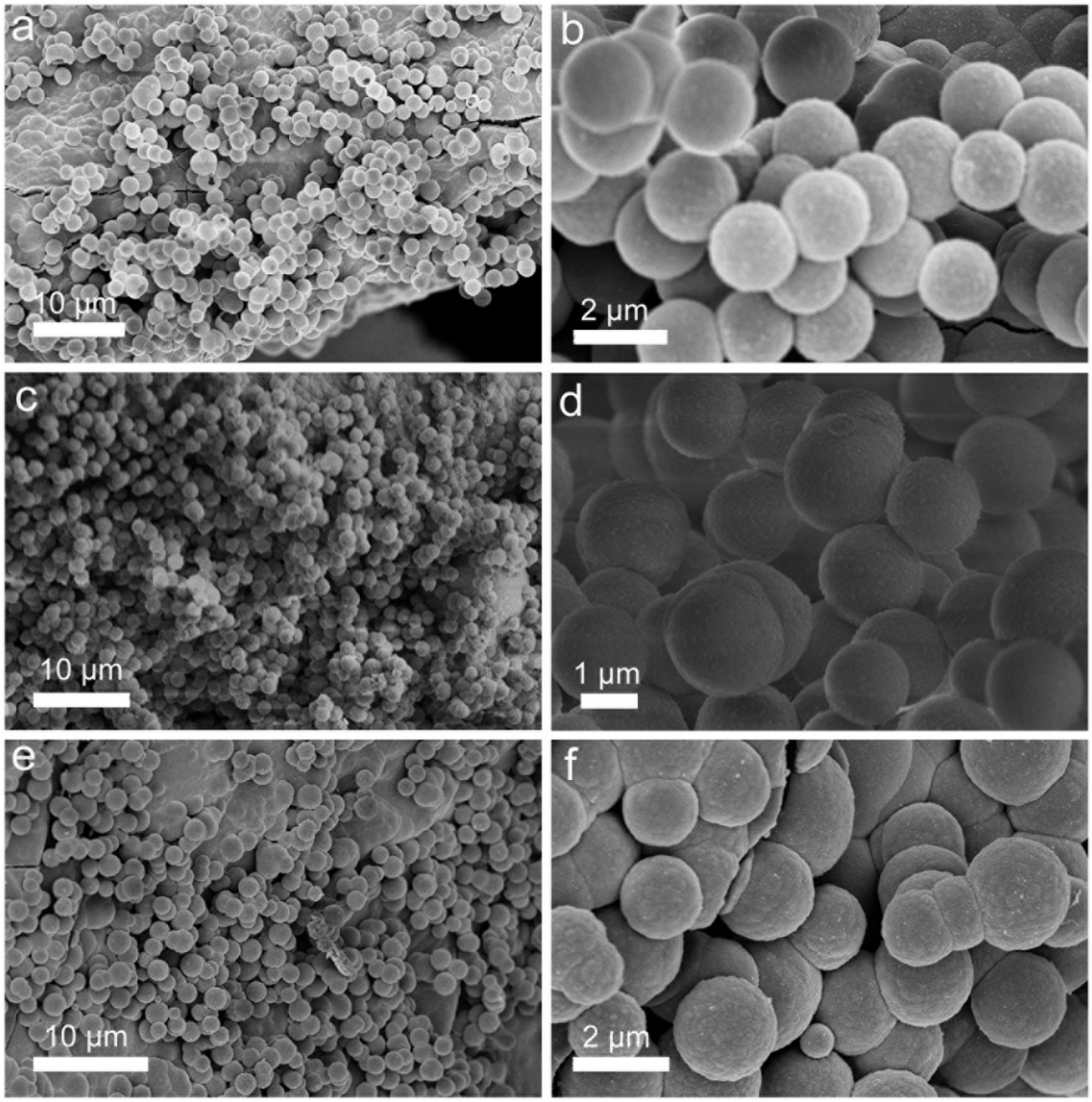

Figure S3. (a), (b): FESEM image of Ni MOF-Fe-1; (c), (d): FESEM image of Ni MOF-Fe-2; (e), (f): FESEM image of Ni MOF-Fe-3.

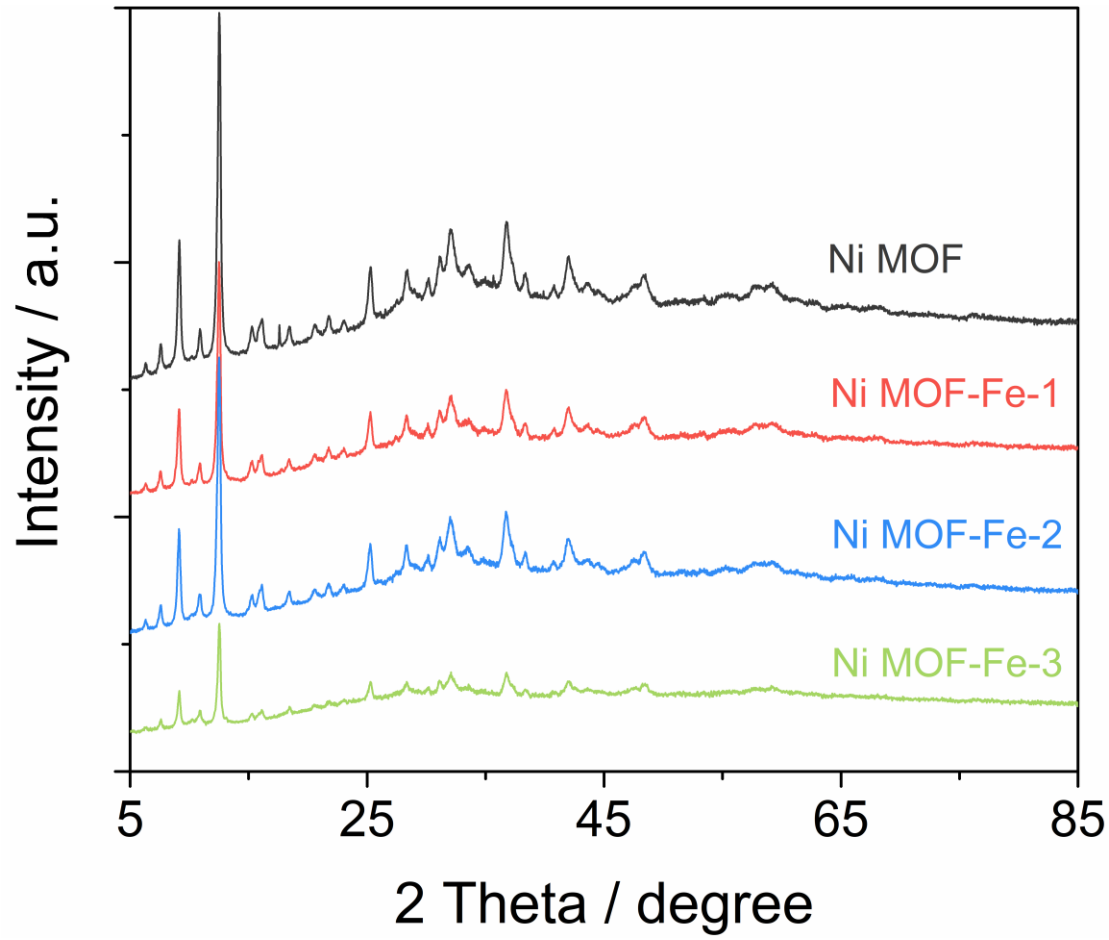

Figure S4. XRD pattern of samples.

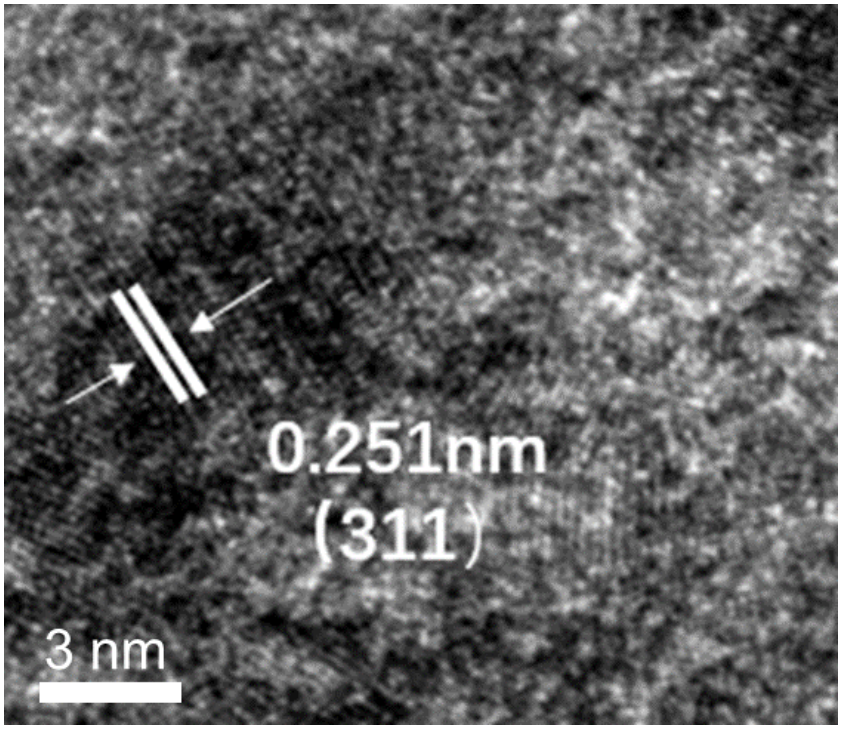

Figure S5. HRTEM image of Ni MOF-Fe-2.

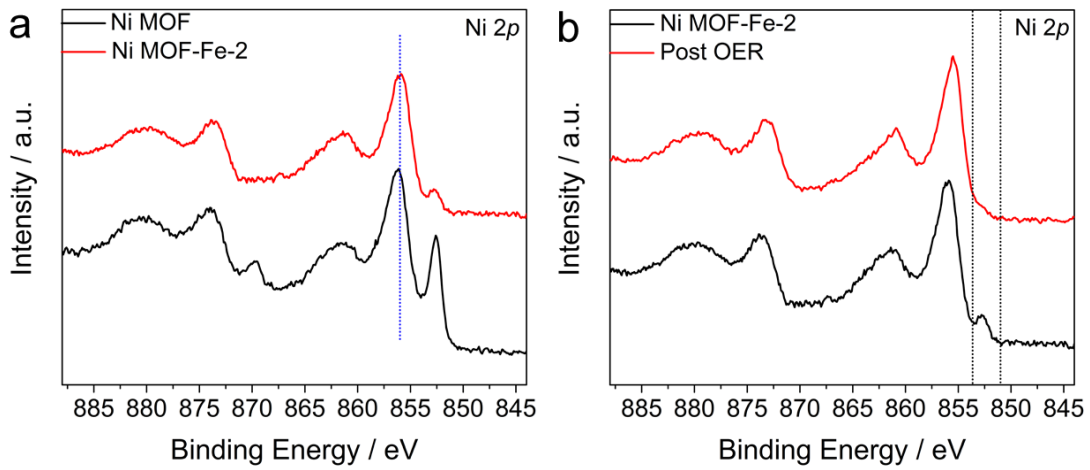

Figure S6. (a): high-resolution Ni 2*p* spectrum of Ni MOF and Ni MOF-Fe-2; (b): High-resolution Ni 2*p* spectra of Ni MOF-Fe-2 before and after OER.

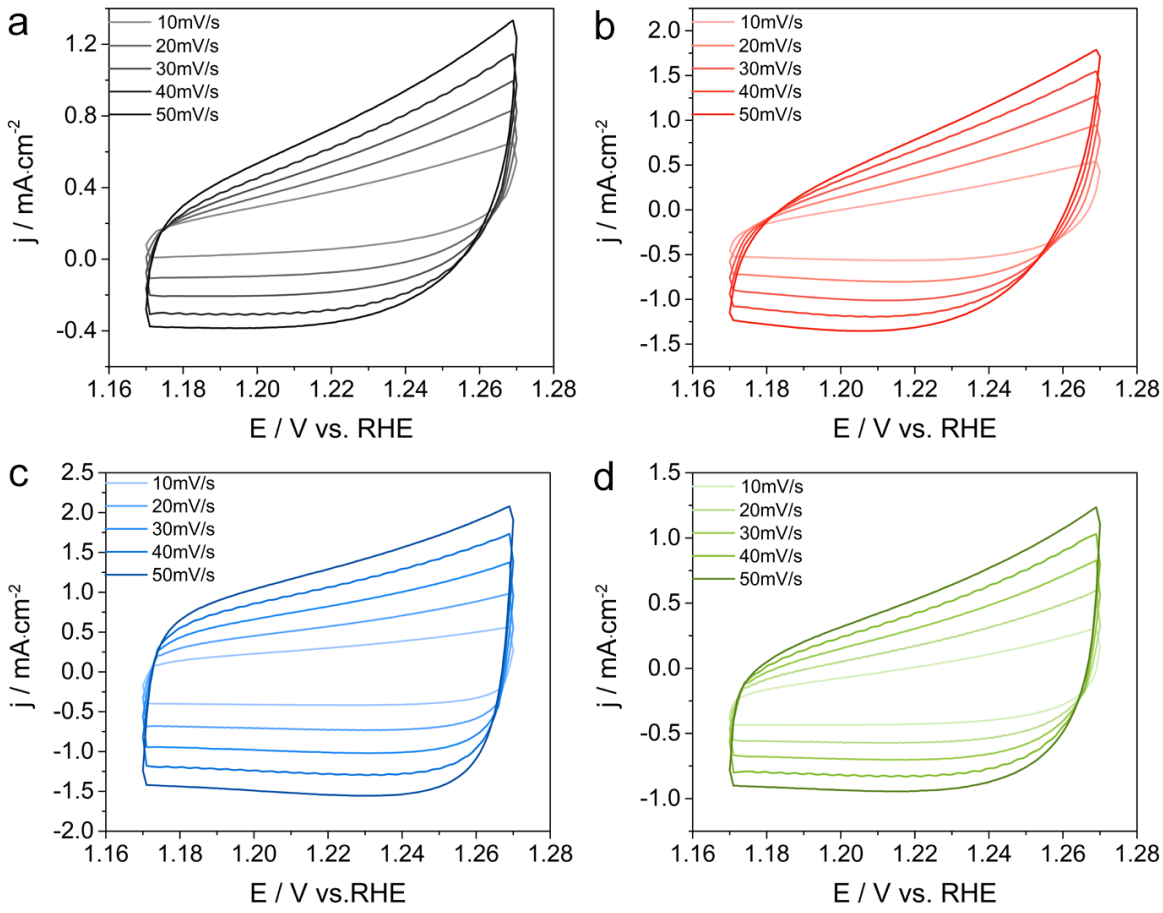

Figure S7. CV curves of (a) Ni MOF, (b) Ni MOF-Fe-1, (c) Ni MOF-Fe-2 and (d) Ni MOF-Fe-3 under potential of 1.17-1.14 V vs RHE at different scan rate.

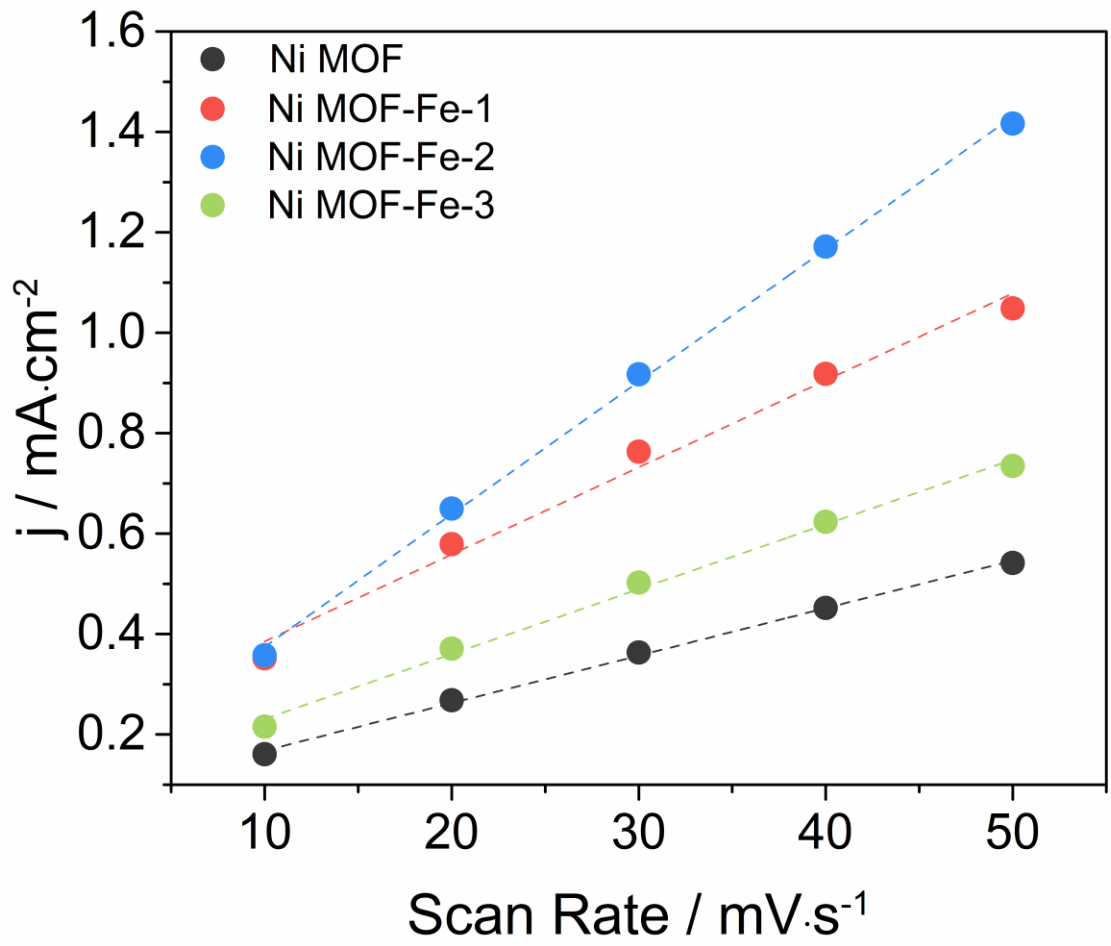

Figure S8. Plot the difference in current density at 1.22V vs. RHE against different scan rates, yielding the double-layer capacitance (C_{dl}) of the samples.

.

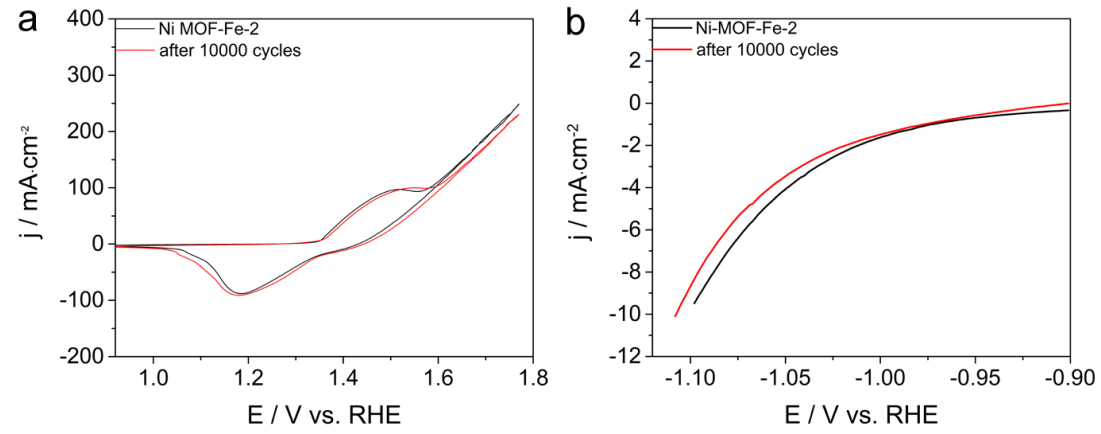

Figure S9. (a): CV curves of Ni MOF-Fe-2 at the 1st and 10000th cycle for OER; (b): Polarization curves of Ni MOF-Fe-2 at the 1st and 10000th cycle for HER.

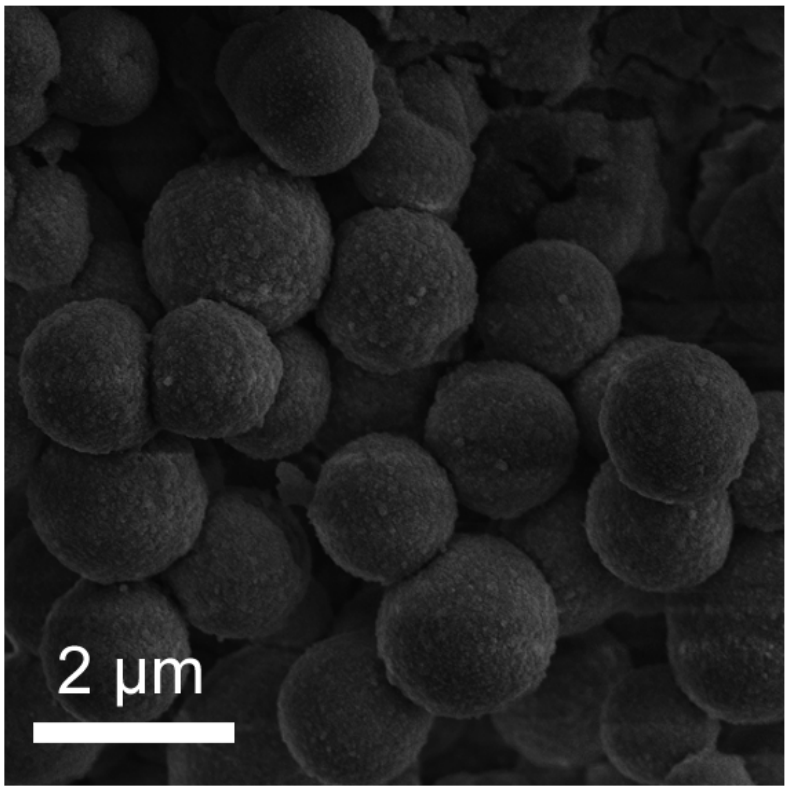

Figure S10. FESEM image of Ni MOF-Fe-2 after OER stability test.

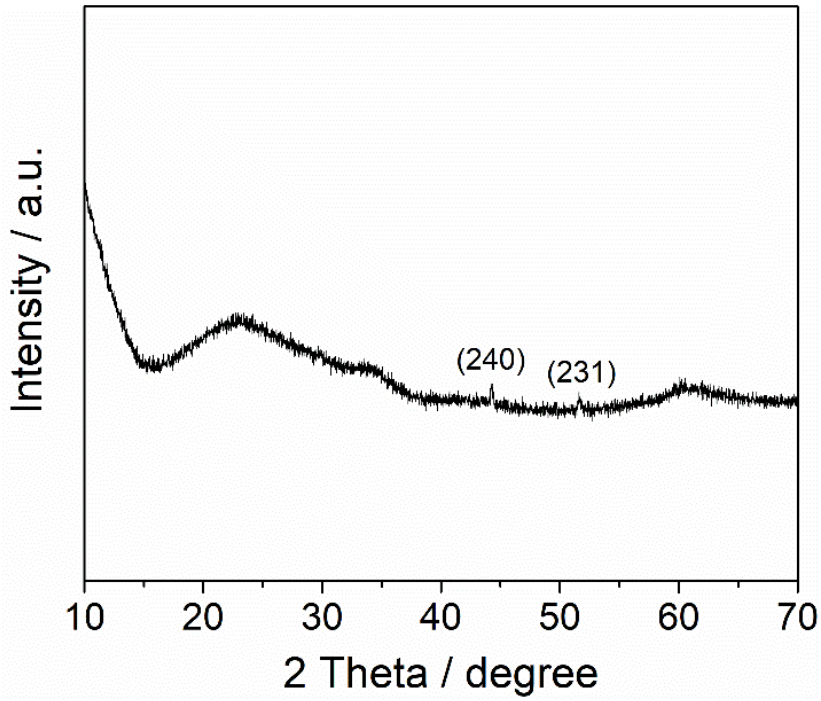

Figure S11. XRD pattern of Ni MOF-Fe-2 after OER stability test.

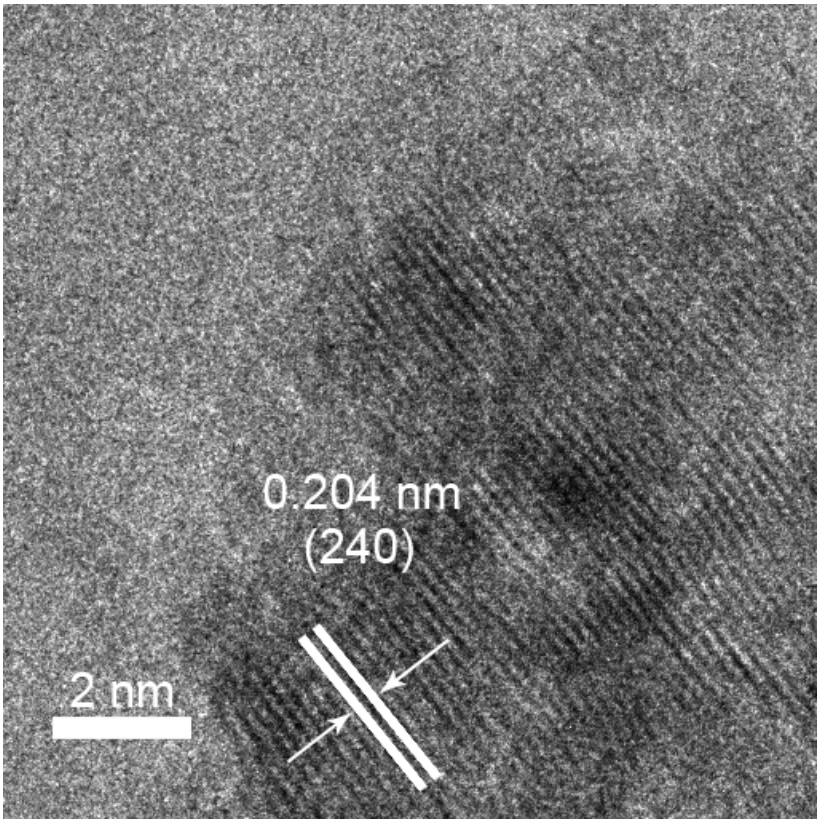

Figure S12. HR-TEM image of Ni MOF-Fe-2 after OER stability test.

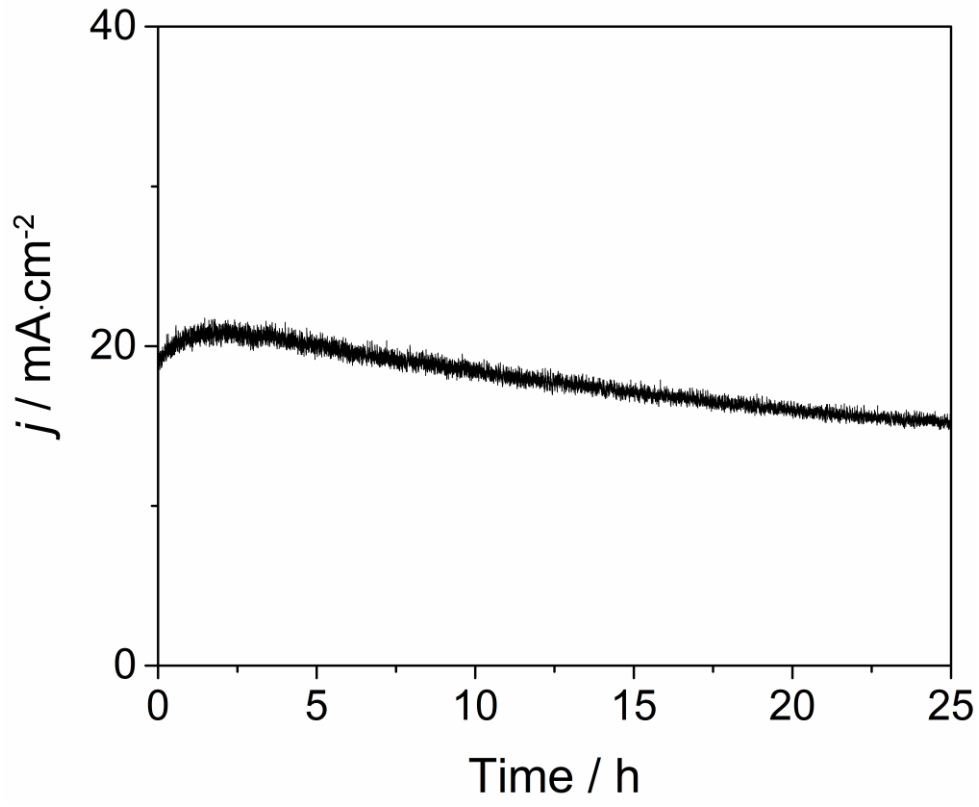

Figure S13. long-term stability test of Ni MOF at 1.5 V vs RHE for 25 h.

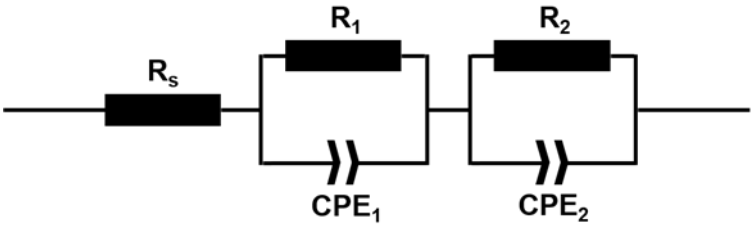

Figure S14. Equivalent circuit used for the fitting of the EIS, where R_s, R_1, R_2, CPE_1, and CPE_2 represent the solution resistance, electrode texture, charge transfer resistances and constant phase elements, respectively.

DFT calculation:

In this work, the density functional theory (DFT) calculation was performed by the Cambridge serial total energy package (CASTEP) code, in which a plane wave basis set was used. The exchange and correlation interactions were modeled using the generalized gradient approximation (GGA) and the Perdew-Burke-Ernzerhof (PBE) functional. The Vanderbilt ultrasoft pseudopotential was used with a cutoff energy of 450 eV. Geometric convergence tolerances were set for maximum force of 0.03 eV/A˚ , maximum energy change of 10^{-5} eV/atom, maximum displacement of 0.001 A˚ and maximum stress of 0.5 GPa. Density mixing electronic minimisation was implemented and the self-consistent field (SCF) tolerance was set to ‘‘fine’’ with high accuracy of 10^{-6} eV/atom for energy convergence.

The key reaction steps in alkaline OER:

According to a previous study on the OER pathway in alkaline media, the OER pathway was described as the adsorption of successive intermediate species on the catalyst and the relevant reaction energies were as follows (*Eq.* 1 ~ *Eq.* 4):

1. $OH^- + cat \rightarrow *OH\text{-}cat + e^-$
2. $*OH\text{-}cat + OH^- \rightarrow *O\text{-}cat + H_2O + e^-$
3. $*O\text{-}cat + OH^- \rightarrow *OOH\text{-}cat + e^-$
4. $*OOH\text{-}cat + OH^- \rightarrow O_2\uparrow + H_2O + e^-$

The ‘‘cat’’ represented the active site when OER occurred. The ‘‘*OH”, ‘‘*O”, ‘‘*OOH” represented the intermediate species adsorbed on the active sites. In order to evaluate OER activity, we calculated the free energy ($\Delta G_1 \sim \Delta G_4$) using the computational standard hydrogen electrode model. The free energy calculation could be obtained as follows:

$$\Delta G_1 = G_{OH\text{-}cat} - G_{cat} - G_{H2O} + 1/2G_{H2} - eU + K_B T Ln10 \cdot pH \quad (1)$$

$$\Delta G_2 = G_{O\text{-}cat} - G_{OH\text{-}cat} + 1/2G_{H2} - eU + K_B T Ln10 \cdot pH \quad (2)$$

$$\Delta G_3 = G_{OOH\text{-}cat} - G_{O\text{-}cat} - G_{H2O} + 1/2G_{H2} - eU + K_B T Ln10 \cdot pH \quad (3)$$

$$\Delta G_4 = 4.92 - \Delta G_1 - \Delta G_2 - \Delta G_3 \quad (4)$$

It should be noted that -eU represented the free energy changes for one electron transfer where U was electrode potential respect to the standard hydrogen electrode. For pH ≠ 0, pH effected on free energy could be defined as $-K_B T Ln10 \cdot pH$, where K_B was Boltzman constant. ΔG_4 was calculated by 4.92 - ΔG1 - ΔG2 - ΔG3 to avoid

calculating the O_2 adsorption and desorption. It was known that the DFT calculation might not accurately describe the free energy of O_2 molecule in the gas phase and hence we used H_2O and H_2 as reference and from there we extracted the free energy of O_2 through the reaction $O_2 + 4(H^+ + e^-) \rightarrow 2H_2O$. The equilibrium potential for this reaction was 1.23 V and since it was a four electron transfer reaction, the full energy was 4 × 1.23 = 4.92 eV. This analysis was based on the scheme developed by Norskov's group. The overpotential of OER in this mechanism was defined as $\eta_{OER} = \max(\Delta G_{OER}/e) - 1.23$ V.

The adsorption energy(E_{ad}) is defined as $E_{ad}=E_{btc(001)+adsorbate} - E_{adsorbate} - E_{btc(001)}$, Where $E_{btc(001)+adsorbate}$ is the total energy of btc(001) adsorbed with *OH, $E_{adsorbate}$ is the total energy of OH^-, $E_{btc(001)}$ is the total energy of btc(001).

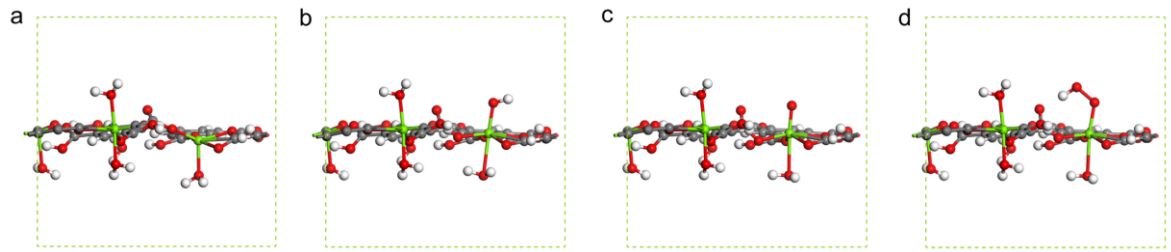

Figure S15. Schematic profile of adsorption oxygen species intermediates on the Ni site in Ni MOF during the OER pathway.

2. Supplementary Tables

Table S1. The proportion of Ni and Ni^{2+} in all nickel elements in the samples

Sample	Ratio of Ni^{2+} / %	Ratio of Ni / %
Ni MOF	52.81	21.57
Ni MOF-F-2	61.1	5.06

Table S2. Comparison of OER performance between Ni MOF-Fe-2 and MOF-derived electrocatalysts reported in recent years

Catalyst	η / mV at 10 mA cm^{-2}	Tafel Slope / mV dec^{-1}	Electrolyte	Reference
Ni MOF-Fe-2	229	37	1.0 M KOH	This work
Co_4Ni_1-P NTs	245	61	1.0 M KOH	1
Co-CNT/PC	315	73.8	0.1 M KOH	2
14.6% CeO_x/CoS	269	50	alkaline	3
Ru@NiCo-MOF HPNs	284	78.8	1.0 M KOH	4
Co_3O_4@CoP	238	51.4	1.0 M KOH	5
Ni_2P-CoP	320	69	0.1 M KOH	6
NI-Fe-MOF NSs	221	56.0	1.0 M KOH	7
$(Ni_2Co_1)_{0.925}Fe_{0.075}$-MOF-NF	257	41.3	1.0 M KOH	8
UTSA-16	408	77	1.0 M KOH	9
NiCoS/$Ti_3C_2T_x$	365	58.2	1.0 M KOH	10
$Co_{0.6}Fe_{0.4}$-MOF-74	280	56	1.0 M KOH	11
Co_3O_4/MoS_2	230	45	1.0 M KOH	12
$A_{2.7}$B-MOF-$FeCo_{1.6}$	288	39	1.0 M KOH	13
$CoSe_2$-450	330	79	1.0 M KOH	14
CNT-NC-CoP	251	82.1	1.0 M KOH	15

Table S3. Difference value of Gibbs free energy of oxygen species intermediates in Ni MOF and Ni MOF-Fe during the OER

Catalyst	ΔG_1 (eV)	ΔG_2 (eV)	ΔG_3 (eV)	ΔG_4 (eV)
Ni MOF (001)	1.89946	1.20516	1.36477	0.4506
Ni MOF-Fe (001)	0.92428	1.40173	1.74867	0.84532

3. Reference

1. L. Yan, L. Cao, P. Dai, X. Gu, D. Liu, L. Li, Y. Wang and X. Zhao, *Advanced Functional Materials*, 2017, **27**, 1703455.
2. S. Dou, X. Li, L. Tao, J. Huo and S. Wang, *Chem Commun (Camb)*, 2016, **52**, 9727-9730.
3. H. Xu, J. Cao, C. Shan, B. Wang, P. Xi, W. Liu and Y. Tang, *Angew Chem Int Ed Engl*, 2018, **57**, 8654-8658.
4. D. Liu, H. Xu, C. Wang, H. Shang, R. Yu, Y. Wang, J. Li, X. Li and Y. Du, *Inorg Chem*, 2021, DOI: 10.1021/acs.inorgchem.1c00295.
5. J. Zhou, Y. Dou, A. Zhou, R.-M. Guo, M.-J. Zhao and J.-R. Li, *Advanced Energy Materials*, 2017, **7**, 1602643.
6. X. Liang, B. Zheng, L. Chen, J. Zhang, Z. Zhuang and B. Chen, *ACS Appl Mater Interfaces*, 2017, **9**, 23222-23229.
7. F. L. Li, P. Wang, X. Huang, D. J. Young, H. F. Wang, P. Braunstein and J. P. Lang, *Angew Chem Int Ed Engl*, 2019, **58**, 7051-7056.
8. Q. Qian, Y. Li, Y. Liu, L. Yu and G. Zhang, *Adv Mater*, 2019, **31**, 1901139.
9. J. Jiang, L. Huang, X. Liu and L. Ai, *ACS Appl Mater Interfaces*, 2017, **9**, 7193-7201.
10. H. Zou, B. He, P. Kuang, J. Yu and K. Fan, *ACS Appl Mater Interfaces*, 2018, **10**, 22311-22319.
11. X. Zhao, B. Pattengale, D. Fan, Z. Zou, Y. Zhao, J. Du, J. Huang and C. Xu, *ACS Energy Letters*, 2018, **3**, 2520-2526.
12. A. Muthurasu, V. Maruthapandian and H. Y. Kim, *Applied Catalysis B: Environmental*, 2019, **248**, 202-210.
13. Z. Xue, Y. Li, Y. Zhang, W. Geng, B. Jia, J. Tang, S. Bao, H.-P. Wang, Y. Fan, Z.-w. Wei, Z. Zhang, Z. Ke, G. Li and C.-Y. Su, *Advanced Energy Materials*, 2018, **8**, 1801564.
14. X. Liu, Y. Liu and L.-Z. Fan, *Journal of Materials Chemistry A*, 2017, **5**, 15310-15314.
15. X. Wang, Z. Ma, L. Chai, L. Xu, Z. Zhu, Y. Hu, J. Qian and S. Huang, *Carbon*, 2019, **141**, 643-651.